nature protocols

PROTOCOL

https://doi.org/10.1038/s41596-018-0001-1

Standardized assays for determining the catalytic activity and kinetics of peroxidase-like nanozymes

Bing Jiang[1,5], Demin Duan[1,5], Lizeng Gao[2,5], Mengjie Zhou[1], Kelong Fan[1], Yan Tang[2], Juqun Xi[2], Yuhai Bi[3], Zhou Tong[3], George Fu Gao[3], Ni Xie[4], Aifa Tang[4], Guohui Nie[4], Minmin Liang[1*] and Xiyun Yan[1*]

Nanozymes are nanomaterials exhibiting intrinsic enzyme-like characteristics that have increasingly attracted attention, owing to their high catalytic activity, low cost and high stability. This combination of properties has enabled a broad spectrum of applications, ranging from biological detection assays to disease diagnosis and biomedicine development. Since the intrinsic peroxidase activity of Fe_3O_4 nanoparticles (NPs) was first reported in 2007, >40 types of nanozymes have been reported that possess peroxidase-, oxidase-, haloperoxidase- or superoxide dismutase–like catalytic activities. Given the complex interdependence of the physicochemical properties and catalytic characteristics of nanozymes, it is important to establish a standard by which the catalytic activities and kinetics of various nanozymes can be quantitatively compared and that will benefit the development of nanozyme-based detection and diagnostic technologies. Here, we first present a protocol for measuring and defining the catalytic activity units and kinetics for peroxidase nanozymes, the most widely used type of nanozyme. In addition, we describe the detailed experimental procedures for a typical nanozyme strip–based biological detection test and demonstrate that nanozyme-based detection is repeatable and reliable when guided by the presented nanozyme catalytic standard. The catalytic activity and kinetics assays for a nanozyme can be performed within 4 h.

Introduction

Nanozymes are inorganic nanomaterials with intrinsic enzyme-like catalytic activity that possess a number of advantageous properties as compared with natural enzymes. Since the first evidence that ferromagnetic NPs have intrinsic peroxidase-like activity was reported in 2007 (ref. [1]), nanozymes quickly aroused attention from a broad spectrum of scientists and technologists because of their high catalytic activity, low cost, high stability and wide range of applications[2]. To date, there are >40 types of nanomaterials that have been found to possess intrinsic enzyme-like activity, including the peroxidase activity of Fe_3O_4 (refs [1,3]), Co_3O_4 (refs [4–6]), Cu_2O (ref. [7]), FeS (ref. [8,9]), CeO_2 (refs [10,11]), $CoFe_2O_4$ (refs [12,13]), $BiFeO_3$ (ref. [14]), $MnFe_2O_4$ (refs [15,16]), CdS[17,18], FeSe[8], FeTe[19] and $ZnFe_2O_4$ NPs[20,21], graphene oxide[22–24], fullerene[25], and carbon nanotubes[26]; oxidase activity of Au[27,28], Pt[22], $CoFe_2O_4$ (ref. [29]), $ZnFe_2O_4$ (ref. [30]), MnO_2 (refs [31–33]), and CeO_2 NPs[34,35]; haloperoxidase activity of V_2O_5 NPs[36]; and superoxide dismutase (SOD) activity of nano-Pt[37,38], fullerene derivatives[39,40] and nanoceria[41–43]. With the emergence of the new concept of 'nanozymology'[44], nanozyme research has now become an emerging new field connecting nanotechnology and biology. This has opened up a broad range of applications for using nanomaterials as biosensors and as tools for diagnosis and treatment.

In contrast to natural enzymes, nanozymes have the following distinct advantages. (i) High stability: inorganic nanomaterials are less fragile than natural enzymes, which allows nanozymes to be used under a wide range of pH (3–12) and temperature (4–90 °C) conditions[44]. By contrast, bioenzymes are generally deactivated under extreme pH and temperature conditions. (ii) Low cost:

[1]Key Laboratory of Protein and Peptide Pharmaceuticals, Institute of Biophysics, Chinese Academy of Sciences, Beijing, China. [2]School of Medicine, Yangzhou University, Yangzhou, China. [3]CAS Key Laboratory of Pathogenic Microbiology and Immunology, Institute of Microbiology, Center for Influenza Research and Early-warning (CASCIRE), Chinese Academy of Sciences, Beijing, China. [4]Institute of Translation Medicine, Shenzhen Second People's Hospital, First Affiliated Hospital of Shenzhen University, Shenzhen, China. [5]These authors contributed equally: Bing Jiang, Demin Duan, and Lizeng Gao. *e-mail: mmliang@ibp.ac.cn; yanxy@ibp.ac.cn

the production process for enzymes is usually complex and expensive, whereas inorganic nanomaterials can be produced easily, with high efficiency, and at low cost. (iii) Cyclic use: Nanozymes are recyclable, with no substantial loss in catalytic activity in subsequent cycles[1,44]. (iv) Easy multifunctionalization: nanozymes have a sufficiently large surface area to allow them to be conjugated to multiple ligands in order to achieve multifunctionalization.

Given these advantages, nanozymes have shown great potential in a broad range of applications. In particular, through the connection of unique physicochemical properties and catalytic activities of nanozymes, many nanozyme-based platform technologies have been developed, with applications in biological detection[12,45,46], disease diagnosis[16,35,36] and medicine development[47,48]. For example, the targeting antibody-conjugated ferromagnetic nanozymes simultaneously provide three functions: target capture, magnetic separation and nanozyme color development for detection[1]. In addition, SOD nanozymes (e.g., nanoceria and nanocarbon particles) were reported to be effective neuroprotective antioxidants in vivo that act by eliminating the accumulation of hydrogen peroxide-induced reactive oxygen intermediates[49].

Nanozyme strips are increasingly used for sensitive target detection after conjugating recognition antibody to the surface of nanozymes. The presence of the captured targets is visualized by the nanozyme-catalyzed color reaction induced by incubating the nanozyme strips with colorimetric substrates. For example, Fe_3O_4 nanozyme strips have been successfully used to detect the Ebola virus with 100× higher sensitivity than that of the conventional colloidal gold-strip method[50].

The catalytic activity of nanozymes is highly dependent on their physicochemical properties, such as morphology, size, composition and surface chemistry. With more and more nanozyme applications being developed, there is an urgent need to establish a standardized protocol to define the nanozyme activity units and characterize their catalytic kinetics. In this protocol, we provide detailed instructions for how to determine the catalytic activity of the commonly used peroxidase nanozymes using standardized assays, allowing for reliable quantification and comparison of different types of nanozymes. These standards will benefit the development of nanozyme-based detection and diagnostic methods, and thus render nanozymes a more powerful tool for a wide range of applications.

Overview of the procedure

In this protocol, we provide step-by-step procedures that allow researchers to determine the catalytic activity of a broad range of peroxidase nanozymes of interest. One can assess the catalytic activity of peroxidase nanozymes can be assessed by determining their ability to oxidize the commonly used peroxidase colorimetric substrates 3,3,5,5-tetramethylbenzidine (TMB), di-azo-aminobenzene (DAB), *o*-phenylenediamine (OPD) and 2,2′-azino-bis-(3-ethylbenzthiazoline-6-sulfonic acid) (ABTS) in the presence of H_2O_2 to provide a color reaction (Steps 1–6) (Fig. 1a,b). In this protocol, we describe how to determine the catalytic activity units of peroxidase nanozymes (Steps 7 and 8) (Fig. 1c,d) and how to characterize their catalytic kinetics (Steps 9–16) (Fig. 2) using the nanozyme-catalyzed colorimetric reaction. Throughout the procedures, we use Fe_3O_4 peroxidase nanozyme as a representative example because ferromagnetic NPs were the first discovered and, to date, are the most widely used nanozymes[1,44]. To demonstrate the broad applicability of this standardized protocol, we further evaluate the catalytic properties of two other commonly used peroxidase nanozymes (i.e., nano-Au and nanocarbon particles) (Fig. 1), as well as those of typical Fe_3O_4 nanozymes with different surface modifications (Supplementary Fig. 1), of various particle sizes (Supplementary Fig. 2) and from different (commercial and custom-made) sources (Supplementary Fig. 3).

Finally, we demonstrate how the nanozyme catalytic standard can be used to significantly improve their detection accuracy by performing a typical peroxidase nanozyme–based strip test for the detection of human influenza A (H1N1) virus (Steps 17–24) (Fig. 3).

Applications

The method described here is, to our knowledge, the first standardized approach for measuring and defining the catalytic activity and kinetics of nanozymes. As nanozymes have been used in a broad spectrum of applications, ranging from biological detection to disease diagnosis and biomedicine development, this standardized method thus has broad applicability. Importantly, the standardized method is convenient to perform in a laboratory using commercially available and low-cost reagents and a commonly used UV/visible spectrometer. Because of its remarkable simplicity and universality, the nanozyme standardized method is currently used regularly by our groups and our collaborators. The commonly used peroxidase nanozymes, including numerous metal oxide NPs (such as Fe_3O_4,

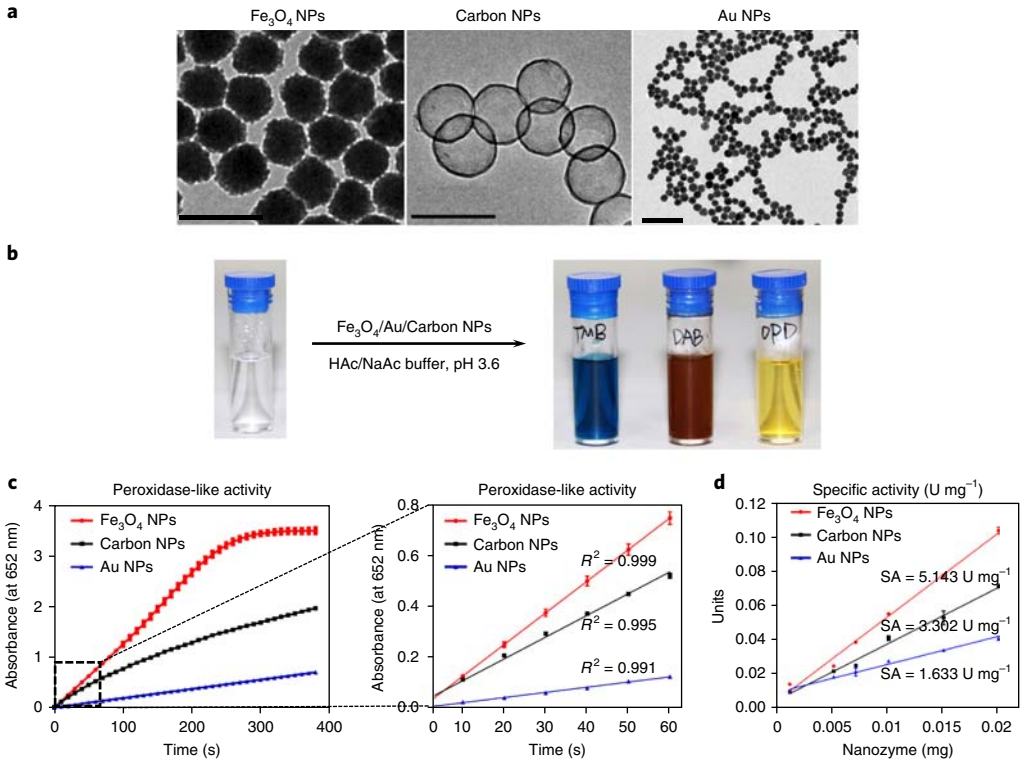

Fig. 1 | Standardization of nanozyme peroxidase-like catalytic activity. a, TEM images of three typical peroxidase nanozymes (Fe_3O_4, carbon and Au NPs). Scale bars represent 200 nm, 200 nm and 100 nm, respectively. **b**, Fe_3O_4, carbon and Au NPs show peroxidase-like activity and catalyze the oxidation of peroxidase substrates (TMB, DAB and OPD) to produce colorimetric reactions. **c**, Left, reaction-time curves of TMB colorimetric reaction catalyzed by Fe_3O_4 (red), carbon (black) and Au (blue) nanozymes. Right, the magnified initial linear portion of the nanozyme reaction-time curves. A length of 60 s was chosen for the initial rate period because the R^2 coefficients were close to 1 during this period after a linear-regression analysis. Absorbance measured in arbitrary units. **d**, The specific activities of Fe_3O_4, carbon and Au nanozymes were calculated as 5.143 U mg^{-1}, 3.302 U mg^{-1} and 1.633 U mg^{-1}, respectively, using the nanozyme activity standardization method described herein. Error bars shown represent s.e. derived from three independent experiments. Values for the individual data points can be found in Supplementary Data 1. SA, specific activity.

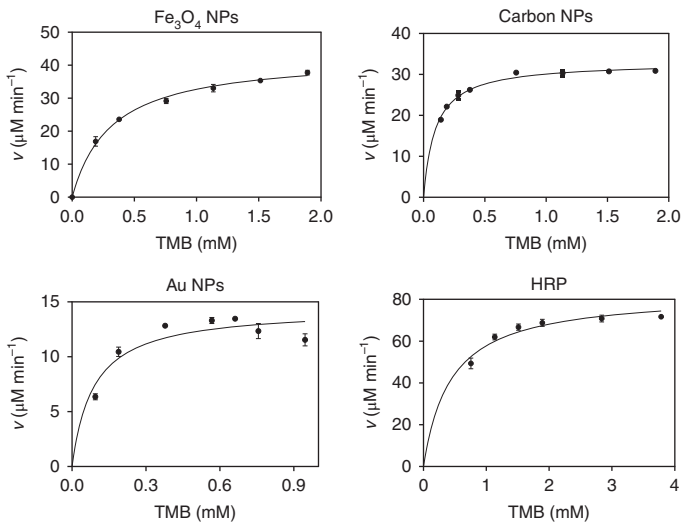

Fig. 2 | Characterization of the catalytic kinetics of peroxidase nanozymes and natural (HRP). Michaelis–Menten curves for Fe_3O_4, carbon and Au nanozymes. The concentration of H_2O_2 used was 1 M, and the TMB concentration varied from 0 to nearly 4 mM. Error bars shown represent the s.e. derived from three independent experiments. Values for the individual data points can be found in Supplementary Data 1. HRP, horseradish peroxidase; *v*, initial reaction velocity.

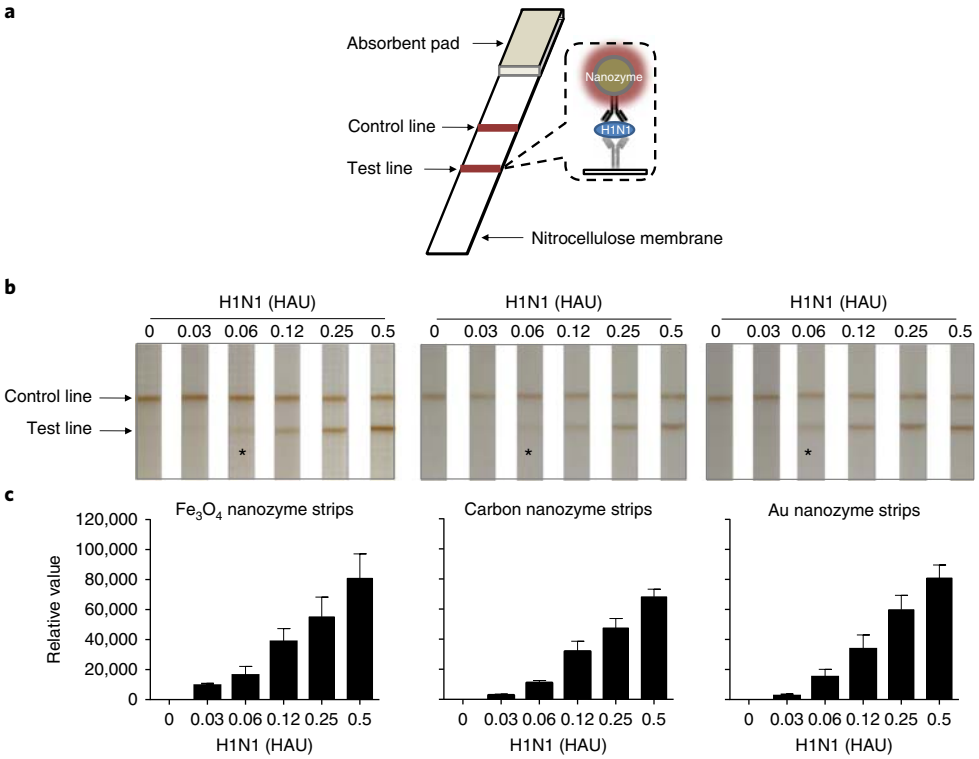

Fig. 3 | Peroxidase nanozyme-based strip method for detecting H1N1 virus with the standardized nanozyme activity units as guide. a, Schematic diagram illustrating the peroxidase nanozyme-based strip detection method. Nanozyme probes catalyze the oxidation of a colorimetric substrate DAB to produce a color reaction at the test line after binding to H1N1 virus particles. The signal intensity of the test line can be visualized qualitatively by the eye and measured quantitatively using a color reader. **b**,**c**, Fe_3O_4, Au and carbon nanozyme-based detection for H1N1 virus (**b**) and the corresponding quantitative results (**c**). Under the guide of the standardized nanozyme catalytic units, consistent detection results were obtained even when different types of nanozymes were used. The asterisks (*) indicate the limit of visual detection of the test line in each strip. HAU values indicate the hemagglutinin titers of H1N1 virus. Error bars shown represent the s.e. derived from three independent experiments. Values for the individual data points can be found in Supplementary Data 1.

Fe_2O_3, Co_3O_4, $CoFe_2O_4$ and $MnFe_2O_4$ NPs), metal NPs (such as Au and Pt NPs) and carbon nanomaterials (such as graphene, carbon NPs and nanotubes) have been tested by this standardized method in our groups.

We have demonstrated the potential of this method to improve the detection accuracy of nanozyme-based methods (Anticipated results). Possible future applications include furthering the fundamental understanding of the catalytic mechanisms of nanozymes to help develop nanozyme-based platform technologies by combining the unique physicochemical properties and catalytic activities of nanozymes. In disease diagnosis and treatment, standardization of nanozyme activity units is expected to lead to a better dosage control while mediating redox-active biological processes (such as those regulating reactive oxygen species in the cancer microenvironment, anti-inflammatory processes, neuroprotection, promotion of stem cell growth and anti-aging processes) using redox-based nanozymes. We previously showed that nanozymes can be used to visualize tumors by immunohistochemical staining of clinical tissues[48] and can help analyze the biodistribution of biomedical NPs in vivo[46]. This further opens novel avenues to nanomedical applications, in which the standardized nanozymes could lead to a better understanding of nanomedicine uptake, biodistribution and pharmacokinetics.

Limitations of the protocol

Over the past decade, along with the remarkable achievements made in the field of nanotechnology, >40 types of nanozymes have been reported to exhibit intrinsic enzyme-like activity, including peroxidase activity, oxidase activity, haloperoxidase activity and superoxide dismutase activity.[44]. The protocol described here specifically presents the standardization of the most widely used type of nanozyme: the peroxidase nanozymes. Hence, this standardized method is not applicable to the

non-peroxidase nanozymes. With more and more applications being developed for non-peroxidase nanozymes, it will be important to establish standardized methods for these in the future as well.

An additional limitation to consider is the possible interference of the NPs themselves (due to their optical properties) in the determination of the absorption intensity of the nanozyme-catalyzed colorimetric reaction. In particular, it is possible that specific classes of NPs absorb near the substrate absorption spectrum. For example, Fe_3O_4 NPs exhibit a specific absorption band in the region of 330–450 nm (ref. [51]), which will severely interfere with the detection of peroxidase nanozyme–catalyzed colorimetric reactions when using OPD (absorption maximum, $\lambda_{max} = 417$ nm) or ABTS ($\lambda_{max} = 420$ nm) as reaction substrates. One way to overcome such interference is by subtracting the background absorbance from the NPs, as described in Step 6 of the Procedure. However, if the interference cannot be excluded by background subtraction, other colorimetric substrates that have no overlapping absorption with the tested NPs should be considered. The commonly used colorimetric substrates include TMB, OPD, ABTS and DAB. Among them, TMB is the most sensitive, because it has a higher molar absorption coefficient ($\varepsilon_{652\ nm} = 39{,}000\ M^{-1}\ cm^{-1}$) than OPD ($\varepsilon_{417\ nm} = 16{,}700\ M^{-1}\ cm^{-1}$) or ABTS ($\varepsilon_{420\ nm} = 36{,}000\ M^{-1}\ cm^{-1}$). DAB is more suitable for immunohistochemical staining or nanozyme strip detection because the brown DAB product catalyzed by nanozymes will quickly precipitate out during reactions that make it difficult to quantitatively detect the nanozyme-catalyzed colorimetric reaction in solution.

Experimental design

Standardization of nanozyme peroxidase-like catalytic activity

In this protocol, one nanozyme activity unit (U) is defined as the amount of nanozyme that catalyzes 1 μmol of product per minute. The specific activity (SA) is defined as activity units per milligram of nanozyme. We provide detailed instructions for how to measure the catalytic activity of peroxidase nanozymes (Steps 1–6) and how to determine their activity units and SA values using the nanozyme-catalyzed colorimetric reaction (Steps 7 and 8). The catalytic activity assays can be performed with the commonly used colorimetric substrates, including TMB ($\varepsilon_{652\ nm} = 39{,}000\ M^{-1}\ cm^{-1}$), OPD ($\varepsilon_{417\ nm} = 16{,}700\ M^{-1}\ cm^{-1}$) and ABTS ($\varepsilon_{420\ nm} = 36{,}000\ M^{-1}\ cm^{-1}$). Here, the nanozyme reaction–time curves can be determined by monitoring the colorimetric response against the reaction time. Usually, one determines the catalytic activities of nanozymes by measuring the slope of the initial linear portion of the nanozyme reaction curves. The catalytic activity of a nanozyme is linearly proportional to its mass. This means that one can determine the SA values of nanozymes by plotting the nanozyme catalytic activities against their weight and measuring the slopes of the resultant straight lines.

Peroxidase nanozymes show high catalytic activity under a wide range of temperatures, whereas natural enzyme horseradish peroxidase (HRP) has an optimal temperature of ~37 °C (Supplementary Fig. 4). To make a valid comparison between nanozymes and natural enzymes, we therefore recommend performing all catalytic assays at 37 °C.

Standardization of the catalytic kinetics of peroxidase nanozymes

The catalytic characterization of nanozymes is dependent on their kinetic constants, which relate reaction rates to substrate concentration according to the Michaelis–Menten equation. We describe the detailed procedures to evaluate the Michaelis–Menten kinetics of peroxidase nanozyme–catalyzed colorimetric reactions in the presence of varying concentrations of colorimetric substrate (Steps 9–13) and to determine their catalytic kinetic constants from the kinetic curves by fitting the reaction velocity values and the initial substrate concentration to the Michaelis–Menten equation (Steps 14–16). With the obtained catalytic kinetics, nanozymes are quantitively compared in terms of the catalytic efficiency (k_{cat}/K_m), substrate specificity (K_m), catalytic rate constant (k_{cat}) and maximal reaction rate (ν_{max}) for specific substrates.

Nanozyme-based detection under the guide of the nanozyme catalytic standard

Because of the complex interdependence of physicochemical properties and catalytic characteristics, nanozyme-based detection applications are severely limited by inferior repeatability and reliability. Here, a typical peroxidase nanozyme–based strip method for the detection of H1N1 virus is used as an example to demonstrate the substantially improved detection accuracy of nanozyme-based methods under the guide of the established nanozyme activity standard (Steps 17–24). In this assay, peroxidase nanozymes catalyze the oxidation of peroxidase substrates to produce an intense color reaction, which is used for quantitative target detection after coupling of recognition antibody to the

surface of nanozymes (Fig. 3a). In the example described in this protocol, anti-H1N1 capture antibodies are immobilized along the test line of the strip, whereas anti-mouse IgG antibodies specific to a second set of anti-H1N1 detection antibodies are immobilized along the control line of the strip. The anti-H1N1 detection antibodies are conjugated to the nanozyme particles, incubated with the (in this case H1N1 virus–containing) sample of interest and incubated with the strip. The detection antibodies–immobilized nanozyme probes are used to catalyze the oxidation of the colorimetric DAB substrate to produce a color reaction at the test line after capturing H1N1 viruses. Whenever the nanozyme probes pass the control line, they will bind to the immobilized anti-mouse IgG antibodies to produce a colored control line. The signal intensity of the test line can be visualized qualitatively by eye or measured quantitatively using a color reader. In this method, the prepared nanozyme detection probes (i.e., anti-H1N1 detection antibody–conjugated nanozymes) are characterized by the number of antibodies per unit of nanozyme and used during detection according to the catalytic activity (in units), instead of the conventional mass or molar concentration, to ensure detection accuracy and repeatability.

Materials

Reagents

- A/California/04/2009 strain of H1N1 (J. Liu, China Agricultural University)
- $FeCl_3 \cdot 6H_2O$ (Sigma-Aldrich, cat. no. F2877)
- $NaAc \cdot 3H_2O$ (Sigma-Aldrich, cat. no. S7670)
- Acetic acid (HAc; Sigma-Aldrich, cat. no. A6283)
- Sodium hydroxide (Sigma-Aldrich, cat. no. S8045)
- Ethanol (Beijing Chemical Reagents, CAS no. 64-17-5) **! CAUTION** Ethanol is highly flammable and should be kept away from flames.
- Glycol (Sigma-Aldrich, cat. no. 293237) **! CAUTION** Glycol is highly flammable and should be kept away from flames.
- 3,3′,5,5′-Tetramethylbenzidine (TMB; Sigma-Aldrich, cat. no. T2885) **! CAUTION** TMB is flammable and toxic upon inhalation, upon contact with skin and if swallowed. Avoid prolonged or repeated exposure. Use in a fume hood and wear gloves, protective eyewear and a lab coat.
- 3,3′-Diaminobenzidine tetrahydrochloride (DAB; Amresco, cat. no. 0430) **! CAUTION** DAB is flammable and toxic upon inhalation, upon contact with skin and if swallowed. Avoid prolonged or repeated exposure. Use in a fume hood and wear gloves, protective eyewear and a lab coat.
- *o*-Phenylenediamine (OPD; Amresco, cat. no. 0688) **! CAUTION** OPD is toxic upon inhalation, ingestion and skin contact. Avoid prolonged or repeated exposure. Wash thoroughly after handling. Use in a fume hood and wear gloves, protective eyewear and a lab coat.
- Hydrogen peroxide, 30% (wt/vol) aqueous solution (Sinopharm Chemical Reagent, CAS no. 7722-84-1) **! CAUTION** Hydrogen peroxide is highly irritating upon contact with eyes or skin, and upon ingestion; It should be handled with gloves under a fume hood.
- Dimethyl sulfoxide (DMSO; Sigma-Aldrich, cat. no. D2650) **! CAUTION** DMSO is harmful if inhaled or absorbed through the skin. It is flammable. DMSO should be used in a fume hood. Wear protective gloves, clothing and a facemask while handling it.
- Antibodies: Anti-H1N1 7304 (Medix Biochemica, cat. no. 100081), anti-H1N1 7307 (Medix Biochemica, cat. no. 100083) and polyclonal goat anti-mouse IgG (Beijing Biodragon Immunotechnologies) **▲ CRITICAL** Store the antibodies at 4 °C only if they are to be used within 1 month. For long-term storage, aliquots can be kept at −80 °C for up to 6 months.
- Horseradish peroxidase (HRP; Sigma-Aldrich, cat. no. P8375)
- 3:1 Poly(4-styrenesulfonic acid-co-maleic acid) sodium salt (Sigma-Aldrich, cat. no. 243051)
- 1-Ethyl-3-(3-dimethylaminopropyl) carbodiimide hydrochloride(Sigma-Aldrich, cat. no. E6383)
- *N*-hydroxysuccinimide (NHS; Sigma-Aldrich, cat. no. 56485)
- BSA (Sigma-Aldrich, cat. no. A2153)
- NaCl (Sinopharm Chemical Reagent, (CAS no.7647-14-5))
- KCl (Sinopharm Chemical Reagent, CAS no. 7447-40-7)
- Na_2HPO_4 (Sinopharm Chemical Reagent, CAS no. 7558-79-4)
- KH_2PO_4 (Sinopharm Chemical Reagent, CAS no.16788-57-1)
- H_3BO_3 (Sinopharm Chemical Reagent, CAS no.10043-35-3)
- $Na_2B_4O_7$ (Sinopharm Chemical Reagent, CAS no.12045-78-2)

- Nitrocellulose membrane (Thermo Fisher Scientific, cat. no. IB301032)
- Tetraethyl orthosilicate (TEOS; Sigma-Aldrich, cat. no. 86578) **! CAUTION** TEOS is flammable and volatile. Handle under a fume hood and wear gloves, protective eyewear and a lab coat.
- $HAuCl_4$ (Sigma-Aldrich, cat. no. 16961-25-4)
- HCl (Sinopharm Chemical Reagents, CAS no.7647-01-0) **! CAUTION** HCl causes severe burns. Do not inhale the vapor. Avoid contact with eyes, skin and clothing. Avoid prolonged or repeated exposure. Use in a fume hood and wear gloves, protective eyewear H_3BO_3 (Sinopharm Chemical Reagents, CAS no. 10043-35-3) $Na_2B_4O_7$ (Sinopharm Chemical Reagents, CAS no. 12045-78-2) and a lab coat.
- HNO_3 (Sinopharm Chemical Reagents, CAS no.7697-37-2) **! CAUTION** HNO_3 causes severe burns. Do not inhale the vapor. Avoid contact with eyes, skin and clothing. Avoid prolonged or repeated exposure. Use in a fume hood and wear gloves, protective eyewear and a lab coat.
- Formaldehyde (Sinopharm Chemical Reagents, CAS no. 50-00-0) **! CAUTION** Formaldehyde is irritating to the eyes and respiratory tract. Handle with gloves under a fume hood and wear protective eyewear and a lab coat.
- Hydrogen peroxide (H_2O_2)
- NP-40 (Abcam,CAS no. 9016-45-9)

Nanoparticles

- 5-nm Fe_3O_4 NPs (Sigma-Aldrich, cat. no. 725331)
- 20-nm Fe_3O_4 NPs (Sigma-Aldrich, cat. no. 725366)
- In-house-made Fe_3O_4, carbon and Au nanoparticles (Supplementary Methods)

Equipment

- UV/visible spectrometer (Hitachi, model no. U-3900)
- Circulating constant-temperature water bath (Beijing Changliu Science and Technology, model no. HX-101), set at 37 °C
- Transmission electron microscope (JEOL, model no. JEM-1400)
- Dynamic light scattering (DLS) instrument (DynaPro-Titan system; Wyatt Technology)
- Forced-air-drying oven (Tianjin Taisite Instrument, model no. 101-2A)
- Nanoparticle-tracking analysis system (Nanosight, model no. NS300)
- Programmable strip cutter (Shanghai Kinbio Tech., model no. ZQ2000) **! CAUTION** The cutter is sharp. Handle it with care.
- Thermometer (Beijing Dihui Technology)
- Biochemistry cultivation cabinet (Shanghai Bluepard Instruments)
- 96-Well U-bottom plate (Corning, cat. no. 2797)
- Immunochramato reader (Shenzhen Highcreation Technology, model no. HR201)
- IsoFlow dispenser (Imagene Technology)
- Color reader (Shanghai Kinbio Tech., model no. DT2050)

Reagent setup

Preparation of Fe3O4 and carbon nanozyme probes

The Fe_3O_4 and carbon nanozyme probes are prepared by conjugation of the anti-H1N1 antibody 7307 to the surface of Fe_3O_4 and carbon NPs (according to ref. [50]). Briefly, dissolve 5 mg each of 1-ethyl-3-(3-dimethylaminopropyl) carbodiimide hydrochloride and NHS in 1 mL of deionized water, and add the mixture to 400 U of Fe_3O_4 or carbon NPs. Incubate the mixture for 30 min 25 °C. Collect the resulting NHS-activated nanozymes by centrifugation at 8,000*g* for 10 min at room temperature and wash them twice with deionized water. Then add 1 mL of anti-H1N1 antibody (100 μg mL^{-1} in PBS buffer) dropwise and incubate the mixture overnight at 4 °C. The conjugates are washed twice with PBS and dispersed into 1 mL of 5% (wt/vol) BSA–PBS solution. ▲ **CRITICAL** Store the Fe_3O_4 and carbon nanozyme probes at 4 °C for a maximum of 3 months.

Preparation of Au nanozyme probes

Adjust 400 U of Au NP solution to pH 8.5 with 0.01 M K_2CO_3. Under gentle stirring, add 1 mL of anti-H1N1 antibody (100 μg mL^{-1} in PBS buffer) dropwise and continue stirring for another 30 min. Block nonspecific binding sites with 5% (wt/vol) BSA–PBS for 10 min. Centrifuge the sample at 8000*g* for 10 min at 4 °C and suspend the product in 1 mL of 5% (wt/vol) BSA–PBS solution. ▲ **CRITICAL** Store the Au nanozyme probes at 4 °C for a maximum of 3 months.

Preparation of nanozyme strips

Nanozyme strips are fabricated according to ref. [49]. Briefly, the test line and control line are dispensed along a nitrocellulose membrane sheet pasted to a vinyl backing (20 cm × 2.5 cm) using an IsoFlow dispenser. The anti-H1N1 antibody 7304 (1.2 mg mL^{-1}) in borate buffer (5 mM, pH 8.8) is dispensed as the test line and the goat anti-mouse IgG antibody (1.0 mg mL^{-1}) in borate buffer (5 mM, pH 8.8) is dispensed as the control line (0.1 μL per 1-mm line). Dry the nitrocellulose membrane sheet at 37 °C for 1 h, then block with 1% (wt/vol) BSA for 30 min. Wash the sheet three times (5 mM borate buffer, pH 8.8) and dry at 37 °C for 3 h. Paste an absorbent pad to the vinyl backing, overlapping with the nitrocellulose membrane sheet. Cut the nitrocellulose membrane sheet into test strips (25 mm × 5 mm) using a strip cutter.

▲ **CRITICAL** Store the nanozyme strips in sealed bags under dry conditions at room temperature for a maximum of 3 years.

H1N1 virus preparation and inactivation

The A/California/04/2009 strain of H1N1 was propagated in 10-d-old specific pathogen–free (SPF) embryonated chicken eggs, and the allantoic fluid was harvested 48–72 h later (see ref. [52] for details). The allantoic fluid with H1N1 was inactivated completely with 0.3% (wt/vol) formaldehyde at 37 °C for 48 h (see ref. [53] for details). The hemagglutinin (HA) titer of the stock viruses was usually ~4 HA units (HAUs), tested by 1% chicken red blood cells with a 96-well V-bottom plate (see ref. [54] for details). The virus can be stored at −80 °C for up to 2 years. **! CAUTION** The active H1N1 virus should be handled in a Biosafety Level 2 (BSL-2) laboratory cabinet. Inactive H1N1 virus can be handled under normal experimental conditions.

TMB/OPD/DAB solution

Dissolve TMB, OPD or DAB in DMSO to a concentration of 10 mg mL^{-1}.

▲ **CRITICAL** The prepared solution should be handled in the dark and used only on the day of preparation.

NaAc–HAc buffer

Prepare a reaction solution containing 0.2 M HAc and 0.2 M NaAc·$3H_2O$ in deionized water, and adjust the final pH to 3.6. The buffer can be stored at 4 °C for up to 3 months.

Borate buffer

Borate buffer is 5 mM H_3BO_3 and 5 mM $Na_2B_4O_7$ in deionized water; adjust the final pH to 8.8.

Equipment setup

DLS instrument

The DynaPro Titan DLS instrument is used to measure the size of nanozymes before and after incubation in Steps 1–5 under the standard reaction conditions. The analysis is performed at 25 °C and the concentration of the samples used is 0.25 mg mL^{-1} in PBS buffer. Measurements are collected at 10-s intervals. Each sample is run ten times.

Procedure

Standardization of nanozyme peroxidase-like catalytic activity ● Timing ~2 h

1 Place 2 mL of a solution containing various amounts (from 0 to 20 μg) of peroxidase nanozyme in 0.2 M NaAc–HAc buffer, pH 3.6 (Reagent setup) in a number of tubes.
▲ **CRITICAL STEP** The catalytic activity of nanozymes is highly dependent on pH. In this assay, the 0.2 M, pH 3.6 NaAc–HAc buffer is optimal for peroxidase nanozymes.

2 Add 100 μL of TMB solution (10 mg mL^{-1} in DMSO) to the vial or test tube and mix.
▲ **CRITICAL STEP** The TMB solution should be handled in the dark and used only on the day of preparation Reagent setup).
▲ **CRITICAL STEP** ABTS (λ_{max} = 420 nm) and OPD (λ_{max} = 417 nm) colorimetric substrates can be used when the tested nanozymes severely interfere with the TMB absorption spectrum.

3 Incubate the reaction mixture in a thermostatic water bath in the dark at a temperature of 37 °C for 1 min. The water bath is connected to the UV/visible spectrometer.

4 Add H_2O_2 to the reaction mixture to a final concentration of 1 M.
▲ **CRITICAL STEP** H_2O_2 should be used fresh to minimize H_2O_2 decomposition. In particular, the H_2O_2 stock solution bottle (30% (wt/vol) aqueous solution from Sigma) should not be open for more than 1 month.

5 In addition to the samples prepared in Step 4, prepare a sample without addition of the H_2O_2 solution. This will serve as the background measurement for Step 6. Mix and react the mixture at 37 °C in the dark, and measure the colorimetric response by absorbance at 652 nm every 10 s for up to 400 s after H_2O_2 addition.

▲ **CRITICAL STEP** Nanozymes show high catalytic activity under a wide range of temperatures (between 30 and 50 °C), whereas natural HRP shows optimal catalytic activity at 37 °C (Supplementary Fig. 4). To make a valid comparison between nanozymes and HRP, all catalytic activity measurements should be performed at 37 °C.

▲ **CRITICAL STEP** Generally, the size of nanozymes should be measured using DLS after this step to monitor whether the tested nanozyme is stable in the reaction solution.

? TROUBLESHOOTING

6 Plot the absorbance at 652 nm against the reaction time to obtain the reaction–time curve (see Fig. 1c (left) for examples).

▲ **CRITICAL STEP** The resulting absorbance should be calculated by subtraction of the background absorbance at 652 nm caused by NPs themselves.

7 Calculate the nanozyme activity (units) using the following equation:

$$b_{\text{nanozyme}} = V/(\varepsilon \times l) \times (\Delta A/\Delta t)$$

where b_{nanozyme} is the catalytic activity of nanozyme expressed in units. One unit is defined as the amount of nanozyme that catalytically produces 1 μmol of product per min at 37 °C; V is the total volume of reaction solution (μL); ε is the molar absorption coefficient of the colorimetric substrate, which is typically maximized at 39,000 M^{-1} cm^{-1} at 652 nm for TMB (the ε values of the other two commonly used substrates are OPD: $\varepsilon_{417\ \text{nm}} = 16{,}700\ M^{-1}\ cm^{-1}$ and ABTS: $\varepsilon_{420\ \text{nm}} = 36{,}000\ M^{-1}\ cm^{-1}$); l is the path length of light traveling in the cuvette (cm); A is the absorbance after subtraction of the blank value; and $\Delta A/\Delta t$ is the initial rate of change in absorbance at 652 nm min^{-1}.

▲ **CRITICAL STEP** For a short period after the start of the reaction, the nanozyme produces product at an initial rate that is approximately linear to the reaction time (Fig. 1c (right)). Therefore, the value of $\Delta A/\Delta t$ (i.e., the slope value in the initial rate period of the nanozyme reaction) is constant, and the calculated b_{nanozyme} value from $\Delta A/\Delta t$ is also a constant. The length of the initial rate period depends on the assay conditions and can range from milliseconds to hours. The length of the initial rate period should be chosen when the R^2 coefficients are close to 1 after a linear-regression analysis.

? TROUBLESHOOTING

8 Calculate the SA of the nanozyme (U mg^{-1}) by

$$a_{\text{nanozyme}} = b_{\text{nanozyme}}/[m]$$

where a_{nanozyme} is the SA expressed in units per milligram (U mg^{-1}) nanozymes, and $[m]$ is the nanozyme weight (mg) of each assay.

▲ **CRITICAL STEP** As the catalytic activity of nanozymes (b_{nanozyme}) is linearly proportional to their mass, determine the a_{nanozyme} value by plotting the catalytic activity of b_{nanozyme} against $[m]$ and measuring the slope of the resultant straight line (Fig. 1d).

Standardization of peroxidase nanozyme catalytic kinetics ● Timing ~2 h

9 Dissolve 10 μg of nanozyme in 2 mL of HAc–NaAc buffer (0.2 M, pH 3.6).

10 Add various volumes (from 0 to 100 μL) of the TMB stock solution (10 mg mL^{-1} in DMSO) to the reaction mixture in various tubes.

▲ **CRITICAL STEP** To obtain a well-fitted Michaelis–Menten curve in Step 13, an appropriate substrate concentration range should be chosen. In the examples discussed in this protocol, we prepared TMB solution with concentrations from 0 to 2 mM. Usually, a suitable substrate concentration range should straddle the K_m value and range roughly from 0.5 × K_m to 5 × K_m.

▲ **CRITICAL STEP** The TMB solution should be handled in the dark and used only on the day of preparation (Reagent setup).

11 Add H_2O_2 to the reaction mixture to a final concentration of 1 M.

▲ **CRITICAL STEP** H_2O_2 should be used fresh to minimize H_2O_2 decomposition. In particular, the H_2O_2 bottle (30% (wt/vol) aqueous solution from Sigma) should not be open for more than 1 month.

12 Mix the samples, place them in a 37 °C water bath and record the initial rate of change of absorbance at 652 nm (i.e., $\Delta A/\Delta t$, relative units of absorbance produced per minute) (Steps 6–8).

13 Convert the rates of absorbance increase to substrate concentrations expressed in micromoles per minute (i.e., the catalytic reaction velocity, ν) and plot this against the substrate concentrations to produce a Michaelis–Menten curve (see Fig. 2 for examples).
▲ CRITICAL STEP To obtain a well-fitted Michaelis–Menten curve, choose an appropriate substrate concentration range.
? TROUBLESHOOTING

14 Calculate the kinetics constants ν_{max} and K_m by fitting the reaction velocity values and the substrate concentrations to the Michaelis–Menten equation as follows:

$$\nu = (\nu_{max} \times [S])/(K_m + [S])$$

where ν is the initial reaction velocity and ν_{max} is the maximal reaction rate that is observed at saturating substrate concentrations. $[S]$ is the concentration of the substrate and K_m is the Michaelis constant. K_m reflects the affinity of the nanozyme for its substrate and is defined as the substrate concentration at half the maximum rate.

15 Calculate the molar concentration of nanozyme in the samples using a nanoparticle-tracking analysis system.
▲ CRITICAL STEP Nanozymes measured should be monodisperse for nanoparticle counting.

16 Calculate the catalytic constant (k_{cat}) using the following equation:

$$k_{cat} = \nu_{max}/[E]$$

where k_{cat} is the rate constant defining the maximum number of substrate molecules converted to product per unit of time. $[E]$ is the nanozyme concentration (M).

Nanozyme-based detection for H1N1 virus ● Timing ~1.5 h

▲ CRITICAL The catalytic activity of nanozymes is highly dependent on their size, morphology, composition and surface chemistry, which consequentially causes individual variability of nanozyme probes and results in unrepeatable detection results. To ensure detection accuracy and reproducibility, antibody-conjugated nanozyme probes should be characterized by the numbers of antibodies per unit of nanozymes.

17 Dissolve the prepared nanozyme probe (i.e., anti-H1N1 detection antibody–conjugated nanozymes; Reagent setup) at a concentration of 1 U μL^{-1} in 50 mM sodium phosphate, pH 7.0, containing 1% (wt/vol) BSA.
▲ CRITICAL STEP The amount of nanozyme probe used for each assay should be added according to the catalytic activity (units) instead of the conventional mass or molar concentration to ensure detection accuracy and repeatability.

18 Add 10 U of nanozyme probe solution and various amounts of H1N1 virus samples from 0 to 0.5 HA titers (HAUs) in 80 μL of reaction buffer (containing 50 mM Tris-HCl, pH 8.0, 150 mM NaCl, 1% (vol/vol) NP-40 and 1% (wt/vol) BSA) and mix well.
! CAUTION H1N1 virus should be handled under inactivated conditions in conventional laboratory environments (Reagent setup).

19 Insert the nanozyme strips (Reagent setup) with anti-H1N1 capture antibody–printed test line and goat anti-mouse IgG antibody-printed control line vertically into the virus sample solution and incubate for 15 min.
▲ CRITICAL STEP Put the strips into the virus sample solution vertically. Make sure that they do not adhere to the reactor wall to prevent the sample solution from quickly spreading and impregnating the strips.
? TROUBLESHOOTING

20 Remove the strips, put them into DAB substrate solution (10 mg mL^{-1} in DMSO) and incubate for ~7 min.
▲ CRITICAL STEP The strips should be incubated in DAB solution for no more than 7 min to avoid high background.
▲ CRITICAL STEP The DAB solution should be handled in the dark and used only on the day of preparation.
? TROUBLESHOOTING

21 Stop color development by washing the strips in deionized water.

22 Visualize the test line by eye.
23 Measure the color intensity of the test lines quantitatively with a color reader.
24 Calculate the mean and standard deviation of the replicate values of all controls and samples.

Troubleshooting

Troubleshooting advice can be found in Table 1.

Table 1 | Troubleshooting

Step	Problem	Possible reason	Solution
5	No obvious absorbance at 652 nm is observed	Decomposition of H_2O_2	H_2O_2 is easily decomposed and should be freshly prepared
7	No constant $\Delta A/\Delta t$ value can be obtained	An inappropriate length was chosen for the initial rate period	Choose the initial linear portion of the reaction-time curve (Fig. 1c (right))
13	No Michaelis–Menten curve can be fitted from the measured data	An inappropriate range of substrate concentrations was chosen	Use a suitable substrate concentration range that should straddle the K_m value and range roughly from 0.5 × K_m to 5 × K_m
19	No obvious control or test line can be visualized on the test strip	The strip adheres to the reactor wall, causing the sample solution to pass the test and control line too quickly to bind with the antibodies printed on the strip	Prevent the test strips from adhering to the reactor wall
20	High background signals are observed	The incubation time in DAB solution is too long	Reduce the incubation time to <7 min

Timing

Reagent setup, preparation of nanozyme probes: 12–15 h for the preparation of Fe_3O_4 or carbon nanozyme probes, and 2 h for Au nanozyme probe preparation
Reagent setup, preparation of nanozyme strips: 5 h
Steps 1–6, measurement of reaction–time curves: 1 h
Steps 7 and 8, calculation of $a_{nanozyme}$ and $b_{nanozyme}$ values: 1 h
Steps 9–13, measurement of Michaelis–Menten kinetics: 1 h
Steps 14–16, calculation of kinetic constants: 1 h
Steps 17 and 18, nanozyme probe solution preparation: 15 min
Steps 19–23, strip test: 30 min
Step 24, data analysis: 30 min

Anticipated results

Figure 1 shows an example of using this protocol to determine the peroxidase-like activity of Fe_3O_4 nanozymes and to calculate their catalytic activity units. Figure 1c shows the typical reaction–time curves of TMB colorimetric reactions catalyzed by Fe_3O_4 nanozymes and Fig. 1d shows the catalytic activity units of Fe_3O_4 nanozymes plotted against the nanozyme mass. These results show that the catalytic activity unit is proportional to the nanozyme mass, yielding a unity slope of 5.143 U mg^{-1} and indicating the SA (i.e., the $a_{nanozyme}$ value expressed as units per milligram of nanozyme) of Fe_3O_4 nanozymes. The specific activities of other two typical peroxidase nanozymes (i.e., Au and carbon NPs) were also measured and calculated by the same procedures, demonstrating a broad applicability of the established nanozyme standardization method.

We further investigated the effect of surface modifications, including those involving SiO_2, polyethylene glycol and dextran, on the catalytic activity of peroxidase nanozymes. As shown in Supplementary Fig. 1, the activity of Fe_3O_4 NPs decreased after surface modification, which may be because the surface-modifying groups shield the surface active sites from their substrates and hence affect the catalytic activity. We also analyzed the standardized catalytic activity of Fe_3O_4 nanozymes of different sizes (i.e., 70, 130 and 250 nm). The results show that the smaller-size Fe_3O_4 NPs exhibit higher activity

Table 2 | Comparison of the kinetic constants of Fe_3O_4, Au and carbon nanozymes and HRP

	[*E*] (M)	K_m (mM)	ν_{max} ($M\ s^{-1}$)	k_{cat} (s^{-1})	k_{cat}/K_m ($M^{-1}\ s^{-1}$)
Fe_3O_4 NPs	2.1×10^{-12}	0.2411	6.55×10^{-7}	3.1×10^{5}	1.30×10^{9}
Carbon NPs	2.2×10^{-11}	0.1037	5.62×10^{-7}	2.6×10^{4}	2.51×10^{8}
Au NPs	3.4×10^{-10}	0.1277	2.75×10^{-7}	8.1×10^{2}	6.34×10^{6}
HRP	6.2×10^{-11}	0.4376	1.38×10^{-6}	2.23×10^{4}	5.10×10^{7}

[*E*] is the enzyme or nanozyme concentration. The molar concentration of nanozymes is determined by a nanoparticle-tracking analysis (NTA) system. K_m is the Michaelis constant, ν_{max} is the maximal reaction velocity and k_{cat} is the catalytic constant, where $k_{cat} = \nu_{max}/[E]$ and the k_{cat}/K_m value indicates the catalytic efficiency of the enzyme or nanozymes.

under the same conditions (Supplementary Fig. 2) due to the greater surface-to-volume ratio of smaller NPs for substrate interaction. In addition, we also standardized the catalytic activity of a set of commercial Fe_3O_4 NPs. The results show the commercial Fe_3O_4 NPs with particle sizes of 5 nm and 20 nm exhibit a higher peroxidase activity than our synthesized large-size Fe_3O_4 NPs (Supplementary Fig. 3), further confirming that the greater surface-to-volume ratio of small NPs results in higher catalytic activity with no limitations to particle sources. In summary, this protocol is universal and suitable for catalytic activity standardization of various peroxidase nanozymes with different components (Fig. 1, Supplementary Data 1), surface modifications (Supplementary Fig. 1), particle sizes (Supplementary Fig. 2) and sources (commercial or lab-made, Supplementary Fig. 3).

In this protocol, a natural peroxidase HRP was used for comparison. When measured using the same procedures, HRP shows an $a_{nanozyme}$ value of 504 U mg^{-1} (Supplementary Fig. 5), which is consistent with the manufacturer's value of >400 U mg^{-1}, indicating the reliability of the standardized methods. As we measured the catalytic activity of both nanozymes and natural enzymes under identical conditions and calculated their activity units using the same equations, the catalytic activities of natural enzymes and nanozymes are thus quantitively compared in terms of $a_{nanozyme}$ values.

In addition, it is important to demonstrate that the observed catalytic activity of nanozymes originates from the NPs themselves and not from dissolved ions as a consequence of the acidic reaction solution. To test this, we incubated the NPs in standard reaction solution (pH 3.6, NaAc–HAc buffer) at 37 °C for 400 s (the time taken for activity measurement), and then removed the NPs from solution by centrifugation. We compared the activity of the leaching solution with that of the collected NPs under the same conditions (Supplementary Fig. 6). The results show that the leaching solution shows almost no catalytic activity, and the observed activity is retained in the collected NPs. To further demonstrate the structural integrity of the tested NPs after the reaction, we performed DLS characterization of the NPs before and after incubation in the reaction solution. The resulting particles are monodispersed with virtually identical diameters before and after incubation (Supplementary Fig. 7). The results indicate that the catalytic activity measurement (i.e., incubation under pH 3.6 reaction conditions for only 400 s) does not affect the structural integrity of the tested particles.

Our approach can be used to quantitatively compare the catalytic characteristics of nanozymes and natural enzymes. Figure 2 shows an example of the measured catalytic kinetics of Fe_3O_4, Au and carbon peroxidase nanozymes using the procedures described in this protocol. A natural HRP was also used here for comparison. By kinetic analysis, these three nanozymes show similar K_m values to those of HRP, reflecting a similar binding affinity for the same reaction substrate. The k_{cat} and k_{cat}/K_m values are considerably different, and a substantially higher value for the Fe_3O_4 nanozyme indicates a higher catalytic efficiency (Table 2).

We also describe how to use the peroxidase nanozyme–based strip method for H1N1 detection following calibration using the standardized nanozyme activity assays. The prepared nanozyme detection probes (i.e., the anti-H1N1 detection antibody–conjugated nanozymes) were characterized by the number of antibodies per unit of nanozyme and were used during detection according to the catalytic activity (U) instead of the conventional mass or molar concentration. The use of the nanozyme activity standard substantially improved the repeatability and reliability of the detection results, even when three different types of nanozyme probes were used (Fig. 3b,c), indicating the necessity of using the standardized activity units for improving the detection accuracy of nanozyme-based methods.

References

1. Gao, L. et al. Intrinsic peroxidase-like activity of ferromagnetic nanoparticles. *Nat. Nanotechnol.* **2**, 577–583 (2007).
2. Kotov, N. A. Inorganic nanoparticles as protein mimics. *Science* **330**, 188–189 (2010).
3. Fu, S. et al. Structural effect of Fe_3O_4 nanoparticles on peroxidase-like activity for cancer therapy. *Colloids Surface B* **154**, 239 (2017).
4. Dong, J. et al. Co_3O_4 nanoparticles with multi-enzyme activities and their application in immunohistochemical assay. *ACS Appl. Mater. Interfaces* **6**, 1959 (2014).
5. Jia, H. et al. Peroxidase-like activity of the Co_3O_4 nanoparticles used for biodetection and evaluation of antioxidant behavior. *Nanoscale* **8**, 5938 (2016).
6. Mu, J., Zhang, L., Zhao, G. & Wang, Y. The crystal plane effect on the peroxidase-like catalytic properties of Co_3O_4 nanomaterials. *Phys. Chem. Chem. Phys.* **16**, 15709–15716 (2014).
7. Guo, Y. et al. Fabrication of Ag-Cu_2O/reduced graphene oxide nanocomposites as SERS substrates for in situ monitoring of peroxidase-like catalytic reaction and biosensing. *ACS Appl. Mater. Interfaces* 9, 19074–19081 (2017).
8. Dutta, A. K. et al. Synthesis of FeS and FeSe nanoparticles from a single source precursor: a study of their photocatalytic activity, peroxidase-like behavior, and electrochemical sensing of H_2O_2. *ACS Appl. Mater. Interfaces* **4**, 1919–1927 (2012).
9. Dai, Z., Liu, S., Bao, J. & Ju, H. Nanostructured FeS as a mimic peroxidase for biocatalysis and biosensing. *Chem. Eur. J.* **15**, 4321–4326 (2009).
10. Celardo, I., Pedersen, J. Z., Traversa, E. & Ghibelli, L. Pharmacological potential of cerium oxide nanoparticles. *Nanoscale* **3**, 1411–1420 (2011).
11. Zhao, H., Dong, Y., Jiang, P., Wang, G. & Zhang, J. Highly dispersed CeO_2 on TiO_2 nanotube: a synergistic nanocomposite with superior peroxidase-like activity. *ACS Appl. Mater. Interfaces* **7**, 6451–6461 (2015).
12. Shi, W., Zhang, X., He, S. & Huang, Y. $CoFe_2O_4$ magnetic nanoparticles as a peroxidase mimic mediated chemiluminescence for hydrogen peroxide and glucose. *Chem. Commun.* **47**, 10785–10787 (2011).
13. Fan, Y. & Huang, Y. The effective peroxidase-like activity of chitosan-functionalized $CoFe_2$ O_4 nanoparticles for chemiluminescence sensing of hydrogen peroxide and glucose. *Analyst* **137**, 1225–1231 (2012).
14. Luo, W. et al. Ultrasensitive fluorometric determination of hydrogen peroxide and glucose by using multiferroic $BiFeO_3$ nanoparticles as a catalyst. *Talanta* **81**, 901–907 (2010).
15. Vernekar, A. A., Das, T., Ghosh, S. & Mugesh, G. A remarkably efficient $MnFe_2O_4$-based oxidase nanozyme. *Chem. Asian J.* **11**, 72–76 (2016).
16. Peng, Y. et al. Size-and shape-dependent peroxidase-like catalytic activity of $MnFe_2O_4$ nanoparticles and their applications in highly efficient colorimetric detection of target cancer cells. *Dalton Trans.* **44**, 12871–12877 (2015).
17. Liu, Q. et al. 5,10,15,20-Tetrakis (4-carboxyl phenyl) porphyrin–CdS nanocomposites with intrinsic peroxidase-like activity for glucose colorimetric detection. *Mater. Sci. Eng. C* **42**, 177–184 (2014).
18. Garai-Ibabe, G., Möller, M., Saa, L., Grinyte, R. & Pavlov, V. Peroxidase-mimicking DNAzyme modulated growth of CdS nanocrystalline structures in situ through redox reaction: application to development of genosensors and aptasensors. *Anal. Chem.* **86**, 10059–10064 (2014).
19. Jiang, L. et al. An ultrasensitive electrochemical aptasensor for thrombin based on the triplex-amplification of hemin/G-quadruplex horseradish peroxidase-mimicking DNAzyme and horseradish peroxidase decorated FeTe nanorods. *Analyst* **138**, 1497–1503 (2013).
20. Liu, W. et al. Paper-based colorimetric immunosensor for visual detection of carcinoembryonic antigen based on the high peroxidase-like catalytic performance of $ZnFe_2O_4$–-multiwalled carbon nanotubes. *Analyst* **139**, 251–258 (2014).
21. Zhao, M. et al. Controlled synthesis of spinel $ZnFe_2O_4$ decorated ZnO heterostructures as peroxidase mimetics for enhanced colorimetric biosensing. *Chem. Commun.* **69**, 7656–7658 (2013).
22. Zhou, Y. et al. Enzyme-mimetic effects of gold@platinum nanorods on the antioxidant activity of ascorbic acid. *Nanoscale* **5**, 1583–1591 (2013).
23. Vineh, M. B., Saboury, A. A., Poostchi, A. A., Rashid, A. M. & Parivar, K. Stability and activity improvement of horseradish peroxidase by covalent immobilization on functionalized reduced graphene oxide and biodegradation of high phenol concentration. *Int. J. Biol. Macromol.* **17**, 32776–32779 (2017).
24. Wang, S. et al. Mimicking horseradish peroxidase and NADH peroxidase by heterogeneous Cu^{2+}-modified graphene oxide nanoparticles. *Nano Lett.* **17**, 2043–2048 (2017).
25. Voeikov, V. L. & Yablonskaya, O. I. Stabilizing effects of hydrated fullerenes C60 in a wide range of concentrations on luciferase, alkaline phosphatase, and peroxidase *in vitro*. *Electromagn. Biol. Med.* **34**, 160–166 (2015).
26. Wang, H. et al. Platinum nanocatalysts loaded on graphene oxide-dispersed carbon nanotubes with greatly enhanced peroxidase-like catalysis and electrocatalysis activities. *Nanoscale* **6**, 8107–8116 (2014).
27. He, W. et al. Au@Pt nanostructures as oxidase and peroxidase mimetics for use in immunoassays. *Biomaterials* **32**, 1139–1147 (2011).
28. Zheng, X. et al. Catalytic gold nanoparticles for nanoplasmonic detection of DNA hybridization. *Angew. Chem. Int. Ed. Engl.* **123**, 12200–12204 (2011).

29. Zhang, X., He, S., Chen, Z. & Huang, Y. $CoFe_2O_4$ nanoparticles as oxidase mimic-mediated chemiluminescence of aqueous luminol for sulfite in white wines. *J. Agric. Food Chem.* **61**, 840–847 (2013).
30. Su, L. et al. Colorimetric detection of urine glucose based $ZnFe_2O_4$ magnetic nanoparticles. *Anal. Chem.* **84**, 5753–5758 (2012).
31. Liu, X. et al. BSA-templated MnO_2 nanoparticles as both peroxidase and oxidase mimics. *Analyst* **137**, 4552 (2012).
32. Yan, X. et al. Oxidase-mimicking activity of ultrathin MnO2 nanosheets in colorimetric assay of acetylcholinesterase activity. *Nanoscale* **9**, 2317 (2017).
33. Liu, J. et al. MnO_2 nanosheets as an artificial enzyme to mimic oxidase for rapid and sensitive detection of glutathione. *Biosens. Bioelectron.* **90**, 69 (2016).
34. Asati, A., Santra, S., Kaittanis, C., Nath, S. & Perez, J. M. Oxidase-like activity of polymer-coated cerium oxide nanoparticles. *Angew. Chem. Int. Ed. Engl.* **48**, 2308 (2009).
35. Asati, A., Kaittanis, C., Santra, S. & Perez, J. M. The pH-tunable oxidase-like activity of cerium oxide nanoparticles achieves sensitive fluorigenic detection of cancer biomarkers at neutral pH. *Anal. Chem.* **83**, 2547–2553 (2011).
36. Natalio, F. et al. Vanadium pentoxide nanoparticles mimic vanadium haloperoxidases and thwart biofilm formation. *Nat. Nanotechnol.* **7**, 530–535 (2012).
37. Paras, J. et al. Helium-based cold atmospheric plasma-induced reactive oxygen species-mediated apoptotic pathway attenuated by platinum nanoparticles. *J. Cell. Mol. Med.* **20**, 1737–1748 (2016).
38. Clark, A., Zhu, A., Kai, S. & Petty, H. R. Cerium oxide and platinum nanoparticles protect cells from oxidant-mediated apoptosis. *J. Nanopart. Res.* **13**, 5547–5555 (2011).
39. Rasouli, V. J., Taghi, M. M., Sarami, F. M. & Mahvash, J. Polyhydroxylated fullerene nanoparticles attenuate brain infarction and oxidative stress in rat model of ischemic stroke. *EXCLI J.* **15**, 378–390 (2016).
40. Hu, Z. et al. Photodynamic anticancer activities of water-soluble C 60 derivatives and their biological consequences in a HeLa cell line. *Chem. Biol. Interact.* **195**, 86–94 (2012).
41. Heckert, E. G., Karakoti, A. S., Seal, S. & Self, W. T. The role of cerium redox state in the SOD mimetic activity of nanoceria. *Biomaterials* **29**, 2705–2709 (2008).
42. Chen, J., Patil, S., Seal, S. & Mcginnis, J. F. Rare earth nanoparticles prevent retinal degeneration induced by intracellular peroxides. *Nat. Nanotechnol.* **1**, 142–150 (2006).
43. Silva, G. A. Nanomedicine: seeing the benefits of ceria. *Nat. Nanotechnol.* **1**, 92–94 (2006).
44. Wei, H. & Wang, E. Nanomaterials with enzyme-like characteristics (nanozymes): next-generation artificial enzymes. *Chem. Soc. Rev.* **42**, 6060–6093 (2013).
45. Liang, M. et al. Fe_3O_4 magnetic nanoparticle peroxidase mimetic-based colorimetric assay for the rapid detection of organophosphorus pesticide and nerve agent. *Anal. Chem.* **85**, 308–312 (2012).
46. Zhuang, J. et al. *Ex vivo* detection of iron oxide magnetic nanoparticles in mice using their intrinsic peroxidase-mimicking activity. *Mol. Pharm.* **9**, 1983–1989 (2012).
47. Ghadi, A., Mahjoub, S., Tabandeh, F. & Talebnia, F. Synthesis and optimization of chitosan nanoparticles: potential applications in nanomedicine and biomedical engineering. *Caspian J. Intern. Med.* **5**, 156 (2014).
48. Fan, K., Cao, C. & Pan, Y. et al. Magnetoferritin nanoparticles for targeting and visualizing tumour tissues. *Nat. Nanotechnol.* **7**, 459–464 (2012).
49. Brynskikh, A. M. et al. Macrophage delivery of therapeutic nanozymes in a murine model of parkinson's disease. *Nanomedicine* **5**, 379–396 (2010).
50. Duan, D. et al. Nanozyme-strip for rapid local diagnosis of Ebola. *Biosens. Bioelectron.* **74**, 134–141 (2015).
51. Sharif, A. et al. Soft template synthesis of super paramagnetic Fe_3O_4 nanoparticles a novel technique. *J. Inorg. Organomet. Polym. Mater.* **19**, 355–360 (2009).
52. Bi, Y. et al. Genesis, evolution and prevalence of H5N6 avian influenza viruses in China. *Cell Host Microbe* **20**, 810–821 (2016).
53. World Organisation for Animal Health. Avian influenza (infection with avian influenza viruses). *OIE Manual of Diagnostic Tests and Vaccines for Terrestrial Animals* Chapter 2.3.4. http://www.oie.int/fileadmin/Home/eng/Health_standards/tahm/2.03.04_AI.pdf (2015).
54. World Health Organization. *WHO Manual on Animal Influenza Diagnosis and Surveillance.* http://www.oie.int/fileadmin/Home/eng/Health_standards/tahm/2.03.04_AI.pdf. (2002).

Acknowledgements

This work was supported by the National Key R&D Program of China (2017YFA0205501), the National Natural Science Foundation of China (81722024, 81571728 and 31530026), the Key Research Program of Frontier Sciences (QYZDY-SSW-SMC013), the Strategic Priority Research Program of the Chinese Academy of Sciences (XDA09030306 and XDPB0304), the Youth Innovation Promotion Association (2014078) and the Sanming Project of Medicine in Shenzhen (SZSM201612031).

Author contributions

M.L. conceived and designed the experiments. B.J., D.D. and L.G. performed the experiments. M.L., B.J., D.D., L.G. and X.Y. reviewed, analyzed and interpreted the data. Y.B., Z.T. and G.F.G. provided the inactivated H1N1 virus. M.L. wrote the paper. B.J., D.D., L.G., M.Z., K.F., Y.T., J.X., Y.B., Z.T., G.F.G., N.X., A.T., G.N., M.L. and X.Y. discussed the results and commented on the manuscript.

Competing interests

The authors declare no competing interests.

Additional information

Supplementary information is available for this paper at https://doi.org/10.1038/s41596-018-0001-1.

Reprints and permissions information is available at www.nature.com/reprints.

Correspondence and requests for materials should be addressed to M.L. or X.Y.

Publisher's note: Springer Nature remains neutral with regard to jurisdictional claims in published maps and institutional affiliations.

Published online: 02 July 2018

Related links

Intrinsic peroxidase-like activity of ferromagnetic nanoparticles: https://doi.org/10.1038/nnano.2007.260
Magnetoferritin nanoparticles for targeting and visualizing tumour tissues: https://doi.org/10.1038/nnano.2012.90
Nanozyme-strip for rapid local diagnosis of Ebola: https://doi.org/10.1016/j.bios.2015.05.025